

Modulated Floquet parametric driving and non-equilibrium crystalline electron states

Egor I. Kiselev,¹ Mark Rudner,^{2,3} and Netanel Lindner¹

¹*Physics Department, Technion, 320003 Haifa, Israel*

²*Department of Physics, University of Washington, Seattle, Washington 98195-1560, USA*

³*Niels Bohr Institute, University of Copenhagen, 2100 Copenhagen, Denmark*

We propose a method to parametrically excite low frequency collective modes in an interacting many body system using an amplitude modulated Floquet drive at optical frequencies. We illustrate this method on the example of terahertz plasmons in a two dimensional electronic system. In the presence of a sufficiently strong drive, plasmons resonant with the modulation frequency become unstable and arrange themselves in a crystal-like structure stabilized by interactions and nonlinearities. The new state breaks the discrete time translational symmetry of the drive as well as the translational and rotational spatial symmetries of the system and exhibits soft, Goldstone-like phononic excitations.

I. INTRODUCTION

The collective modes of a many-body system fingerprint the symmetries underlying a phase of matter. They also play an important role in transitions to non-equilibrium states when the system is subjected to an external drive. In particular, resonantly driving collective modes can lead to instabilities, beyond which new symmetry breaking non-equilibrium states emerge [1–5]. An example for such an instability in classical physics are Faraday waves formed by parametrically driven surface waves [6–8].

Accessing this type of phenomenon in electronic systems is challenging due to a lack of methods for the control and manipulation of collective modes in solids. At the same time, the possibility holds a lot of promise for applications in fields like plasmonics or spintronics. Here, we show that Floquet engineering, which employs driving at optical frequencies to manipulate electronic bandstructures [9–37], can be an effective tool to control collective modes. In particular, we show that off-resonant driving can induce a parametric instability of the plasmon modes via a mechanism we call “modulated Floquet parametric driving” (MFPD), leading to an emergent non-equilibrium state with spatio-temporal correlations that break time and space translation symmetry. To illustrate MFPD, we consider a slow and periodic modulation of a higher frequency drive, which parametrically couples to the soft terahertz (THz) plasmons of two dimensional (2D), Coulomb interacting system driven by circularly polarized light.

We predict a non-equilibrium phase which results from an instability of plasmons driven by the periodic amplitude modulation of the high-frequency driving field. As illustrated in Fig.1 a), the high-frequency Floquet driving results in an altered shape of the quasi-energy bands (red curves). In particular, the effective mass m^* of electrons at the Fermi surface changes. This change results in an altered plasmon dispersion. A periodic modulation of the Floquet drive’s amplitude (Fig.1 b)) results in a periodically changing mass that parametrically excites plasmon modes. For sufficiently strong driving, plasmons with

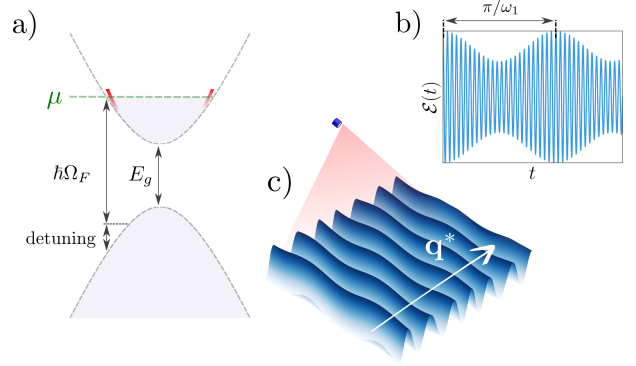


Figure 1. Modulated Floquet parametric excitation of 2D plasmons: a) Illustration of the quasi-energy bands of electrons in a gapped system under MFPD. The dashed gray lines represent the undriven band structure. A Floquet signal with the frequency Ω_F , where $\hbar\Omega_F > E_g$, is applied. The quasi-energy bands in the vicinity of the Fermi surface for a non-zero driving amplitude are shown in red. By altering the amplitude of the Floquet drive, the dispersion and the effective mass of the electrons at the Fermi level is changed. Single photon excitations are blocked by the detuning condition $\mu > \hbar\Omega_F$ (for symmetric particle and hole bands) b) A fast Floquet signal with frequency Ω_F whose amplitude is slowly modulated with the frequency $2\omega_1$. c) The oscillation of the effective electron mass (see Eq. (10)) parametrically excites THz plasmons. Due to nonlinear and interaction effects, the plasmons arrange themselves in a crystal-like structure (shown in blue) whose periodicity is determined by the condition $\omega_1 = \omega_{pl}(q^*)$, where $\omega_{pl}(q)$ is the plasmon dispersion. The crystalline state breaks the rotational and translational symmetries of the undriven system and supports soft phonon-like Goldstone modes which are shown in the figure as small deviations from the plane wave structure of the plasmon lattice.

wavenumbers q^* meeting the condition $\omega_{pl}(q^*) = \omega_1$, where $\omega_{pl}(q)$ is the plasmon dispersion and $2\omega_1$ is the modulation frequency, become unstable and, after a short period of exponential growth, form a crystal-like lattice with a periodically modulated electron density (Fig.1 c)). The structure of this crystal is determined by the nonlinearities of the system. The density oscillates at half

the modulation frequency, thus breaking the π/ω_1 discrete time translation symmetry of the drive – a behavior known from discrete time crystals [38–42].

An important challenge in Floquet engineered systems is heating [43–57]. Here, we show that the parametric excitation of plasmons by MFPD can be achieved in an off-resonant regime where (momentum conserving) single-photon excitation of electrons is blocked. To achieve this, the drive Frequency Ω_F and the Fermi energy μ must be chosen such that all electronic states supporting a resonant interband single photon excitation with an energy transfer of $\hbar\Omega_F$ and near-zero momentum transfer lie below the Fermi surface (see Fig. 1). Processes involving multiple photons are suppressed in the ratio of drive amplitude and drive frequency, leading to strongly reduced heating rates due to photoexcited electrons.

Below, we describe in more detail the excitation of plasmonic instabilities by MFPD, the transition into the crystalline state and the propagation of Goldstone-like, phononic collective modes in the symmetry broken state.

II. EQUATIONS OF MOTION FOR COLLECTIVE DYNAMICS

To describe the electron dynamics, the onset of instability, and the transition to the broken symmetry state, we use a hydrodynamic description of Coulomb interacting electrons (see e.g. [58–60]). The equations of motion follow from the conservation of charge and momentum [61–63]. The continuity equation for the electron density ρ is

$$\partial_t \rho(t, \mathbf{x}) = -\partial_i \rho(t, \mathbf{x}) u_i(t, \mathbf{x}), \quad (1)$$

where $\mathbf{u}(t, \mathbf{x})$ is the electron flow velocity. The continuity equation for the momentum density is given by the Euler equation

$$\partial_t m^* \rho u_i + \partial_j \Pi_{ij} = -\gamma m^* \rho u_i - e \rho \partial_i \phi, \quad (2)$$

where $m^* = \hbar k_F / v_F$ is the effective mass of electrons at the Fermi surface given by the ratio of Fermi momentum $\hbar k_F$ and Fermi velocity v_F , u_i is the electron flow velocity, and γ is the rate of momentum relaxation, e.g. due to impurity or phonon scattering. The stress tensor Π_{ij} is given by

$$\Pi_{ij} = m^* \rho u_i u_j + \delta_{ij} p, \quad (3)$$

where p is the pressure. The electrostatic potential is given by

$$\phi(t, \mathbf{x}) = \int d^2 x' \frac{e \rho(t, \mathbf{x}')}{\varepsilon |\mathbf{x} - \mathbf{x}'|}. \quad (4)$$

Here e is the electron charge and ε the dielectric constant. Solutions of equations (1) and (2) describe the collective oscillations of the electron fluid. In the next section, we discuss how periodic driving can be used to modify the value of the electron mass m^* in these equations, and to realize MFPD.

III. MODULATED FLOQUET PARAMETRIC DRIVING AND CRYSTALLIZATION

A. Modulated Floquet parametric driving

The idea of MFPD is to use the dependence of the quasi-energy band structure on the parameters of the drive to couple to the soft collective modes of the system. Here, we show how the slow modulation of the driving amplitude leads to a time-varying effective electron mass. For concreteness, let us consider a coherently driven, gapped 2D Dirac system described by the Hamiltonian

$$H = \sum_{\mathbf{k}} \mathbf{c}_{\mathbf{k}}^\dagger [H_0(\mathbf{k}) + H_d(t)] \mathbf{c}_{\mathbf{k}} + \sum_{\mathbf{q}} V(\mathbf{q}) \hat{\rho}_{\mathbf{q}} \hat{\rho}_{-\mathbf{q}}. \quad (5)$$

We consider how the external drive modifies the dispersion in a single valley. The dispersion in the opposite valley is modified similarly. Both valley will be taken into account when considering the collective modes. For small values of \mathbf{k} around the center of the valley, we have $H_0 = \mathbf{d} \cdot \boldsymbol{\sigma}$, where $\mathbf{d} = [\lambda k_x, \lambda k_y, E_g/2]$ and $\boldsymbol{\sigma}$ is a Pauli matrix vector describing the orbital pseudospin degree of freedom. E_g is the energy gap between the two bands, $\mathbf{c}_{\mathbf{k}}^\dagger$ ($\mathbf{c}_{\mathbf{k}}$) are electron creation (annihilation) operators and $H_d(t) = e \mathbf{A}(t) \cdot \nabla_{\mathbf{k}} H_0$ is the driving Hamiltonian derived from minimal coupling.

We assume circularly polarized light with an amplitude \mathcal{E} described by $\mathbf{A}(t) = (\mathcal{E}/\Omega) [-\sin \Omega_F t, \cos \Omega_F t, 0]$. The 2D Fourier transform of the Coulomb potential is given by $V(\mathbf{q}) = 2\pi/q$ and $\hat{\rho}_{\mathbf{q}} = \sum_{\mathbf{k}} \mathbf{c}_{\mathbf{k}}^\dagger \mathbf{c}_{\mathbf{k}+\mathbf{q}}$ is the density operator. We emphasize that we use the gapped Dirac Hamiltonian of Eq. (5) as an example. The physics presented here does not depend on the precise band structure of the system.

It is convenient to work in a rotating frame defined by the unitary transformation $U(t) = e^{i \mathbf{d} \cdot \boldsymbol{\sigma} \Omega_F t}$, where the spectrum of the transformed single-particle part of Eq. (5) is given by

$$\varepsilon_{\mathbf{k}} \approx \sqrt{\left(|\mathbf{d}| - \hbar \frac{\Omega_F}{2}\right)^2 + \frac{e^2 \mathcal{E}^2 \lambda^2}{4 \Omega^2 \hbar^2} \left(2 - \frac{E_g}{|\mathbf{d}|}\right)} \quad (6)$$

for $\lambda k / |\mathbf{d}| \ll 1$, we neglected time dependent terms in the rotating frame [11]. In this frame and with the made approximations, the time dependence caused by the fast Ω_F oscillation of the Floquet drive does not explicitly appear in the equations.

We consider the metallic regime with the Fermi surface lying in the upper band (see Fig. 1) and expand the spectrum around k_F – the Fermi momentum of the undriven system. We write:

$$\varepsilon_{\mathbf{k}} \approx \hbar v_F(\mathcal{E}, \Omega_F) (k - k_F) + \varepsilon_{k_F}(\mathcal{E}, \Omega_F) \quad (7)$$

The Fermi velocity $v_F(\mathcal{E}, \Omega_F)$ depends on the amplitude and frequency of the Floquet drive.

A variation of the drive amplitude \mathcal{E} results in a small change of the dispersion $\varepsilon_k \rightarrow \bar{\varepsilon}_k + \delta\varepsilon_k$ near the Fermi surface. To clearly distinguish between constant quantities and quantities oscillating with the slow modulation frequency ω_1 , here and in the following, we write the constant part with a bar. The total charge of the system is conserved and therefore k_F is fixed, however, the slope of ε_k at k_F and therefore the effective mass of the electrons $m^* = \hbar k_F / v_F(\mathcal{E}, \Omega_F)$ are altered. For a small $\delta\varepsilon_k$, we find

$$\bar{\varepsilon}_k + \delta\varepsilon_k \approx \left(1 - \frac{\delta m^*}{\bar{m}^*}\right) \frac{\hbar^2 k_F}{\bar{m}^*} (k - k_F). \quad (8)$$

We consider a slow, adiabatic oscillation of the electric field amplitude \mathcal{E} ,

$$\mathcal{E}(t) = \bar{\mathcal{E}} + \delta\mathcal{E} \cos(2\omega_1 t), \quad (9)$$

such that $\omega_1 \ll \Omega_F$. This slow oscillation does not couple to any single-electron degrees of freedom. However, as demonstrated below, it does couple to the soft plasmon mode through a parametric resonance induced by the periodic change of the effective mass

$$m^*(t) = \bar{m}^* \left(1 + \frac{\delta m^*(t)}{\bar{m}^*}\right). \quad (10)$$

B. Instability

The oscillating mass increment $\delta m^*(t)$ in Eq. (2) acts as a parametric drive, which is known to lead to instabilities [64]. In the following we identify the parametric instability of the charge density ρ . It is convenient to take the divergence of Eq. (2) and to combine the result with the continuity equation (1), including the drive-induced temporal modulation of $m^*(t)$. We find

$$\partial_t m^*(t) \partial_t \rho + \gamma m^*(t) \partial_t \rho - m^*(t) \partial_i \partial_j \rho u_i u_j = \partial_i \rho \partial_i \phi, \quad (11)$$

where we neglected the pressure term p in Eq. (11) since its contribution is subleading to the long-range Coulomb potential [65, 66] [67]. In what follows, we will also neglect the time dependent contribution to the damping term, which is negligible in comparison to the static one.

We proceed with the linear stability analysis of Eq. (11). Writing $\rho = \bar{\rho} + \delta\rho$, where $\delta\rho$ is a small perturbation of the background charge density $\bar{\rho}$, and performing a Fourier transform in the spatial variables, to linear order in $\delta\rho$ we obtain

$$\partial_t (1 + h \cos(2\omega_1 t)) \partial_t \delta\rho_q + \gamma \partial_t \delta\rho_q + \omega_{\text{pl}}^2(q) \delta\rho_q = 0, \quad (12)$$

where we have abbreviated $\delta m^*(t) / \bar{m}^* = h \cos(2\omega_1 t)$ and where $\omega_{\text{pl}}(q)$ is the plasmon dispersion

$$\omega_{\text{pl}}(q) = \sqrt{\frac{2\pi e^2 \bar{\rho} q}{\varepsilon \bar{m}^*}}. \quad (13)$$

Exponentially growing solutions for $\delta\rho_q$, with a growth rate proportional to the dimensionless mass modulation amplitude h , indicate unstable modes.

We first solve Eq. (12) in the vicinity of the resonance $\omega_{\text{pl}}(q) = \omega_1$ with the slowly varying envelope approximation [64]. We will then consider how the driving modifies the plasmon dispersion away from the resonance. The ansatz

$$\delta\rho_q = a_q(t) \cos(\omega_1 t) + b_q(t) \sin(\omega_1 t), \quad (14)$$

when used in Eq. (12), leads to the two equations

$$\begin{aligned} -\frac{1}{2}\omega_1^2 h b_q - 2\dot{a}_q \omega_1 - \gamma a_q \omega_1 + (\omega_{\text{pl}}^2(q) - \omega_1^2) b_q &= 0 \\ \frac{1}{2}\omega_1^2 h a_q + 2\dot{b}_q \omega_1 + \gamma b_q \omega_1 + (\omega_{\text{pl}}^2(q) - \omega_1^2) a_q &= 0, \end{aligned} \quad (15)$$

where we neglected the second derivatives of a_q and b_q , as they are of higher order in the small h around $\omega_{\text{pl}}(q) = \omega_1$. Assuming $a = a(0) e^{s(q)t}$, $b = b(0) e^{s(q)t}$, we find

$$s_{\pm}(q) = -\frac{\gamma}{2} \pm \frac{\omega_1}{2} \sqrt{\left(\frac{h}{2}\right)^2 - \frac{(\omega_{\text{pl}}^2(q) - \omega_1^2)^2}{\omega_1^4}}. \quad (16)$$

The instability condition $\text{Re}(s) > 0$ is realized for $h > 2\gamma/\omega_1$ in a narrow frequency range around $\omega_{\text{pl}}(q) = \omega_1$ given by

$$(\omega_{\text{pl}}^2(q) - \omega_1^2)^2 < \omega_1^4 h^2 / 4 - \omega_1^2 \gamma^2. \quad (17)$$

The fastest growing modes have wavenumbers q^* , which are determined by the condition

$$\pm \omega_{\text{pl}}(q^*) = \omega_1. \quad (18)$$

Thus, the parametric driving will excite plasmons with the frequency ω_1 , whose amplitude will grow according to $\delta\rho_{q^*} \sim e^{(h\omega_1/4 - \gamma/2)t}$. Notice that the system's response breaks the discrete time symmetry of the drive with respect to translations by $T = \pi/\omega_1$.

To obtain the full plasmon dispersion in the presence of parametric driving it is convenient to rewrite Eq. (14). According to Floquet's theorem, any solution to Eq. (12) can be written in the form $\delta\rho_q = e^{i\Lambda(q)t} u_{\Lambda}(t)$, where $u_{\Lambda}(t + \pi/\omega_1) = u_{\Lambda}(t)$. Comparing this form of the solution with the one in Eq. (14), we obtain the correspondence between $\Lambda(q)$ and $s(q)$:

$$\Lambda_{\pm}(q) = -is_{\pm}(q) + i\omega_1. \quad (19)$$

The function u_{Λ} is given by $u_{\Lambda}(t) = [a_{\Lambda}(0)(1 + e^{-2i\omega_1 t}) - ib_{\Lambda}(0)(1 - e^{-2i\omega_1 t})] / 2$. Note, that the Floquet exponent $\Lambda(q)$ is defined modulo $2\omega_1$. In terms of the Bloch theory of electronic band structure, $2\omega_1$ plays the role of a reciprocal lattice vector. Eq. (19) is valid near $\omega_{\text{pl}}(q) = \omega_1$. For small q , keeping higher order derivatives in Eq. (15), and neglecting damping,

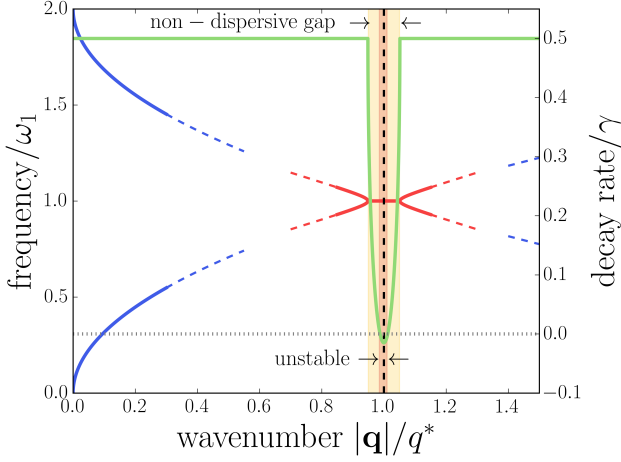


Figure 2. Onset of the plasmon instability induced by modulated Floquet parametric driving with the modulation frequency $2\omega_1$. Red and blue lines show the the quasi-energy dispersion $\text{Re}[\Lambda(q)]$ of parametrically driven plasmons (see Eq. (19) and discussion below). Far away from the critical q^* , 2D plasmons retain the characteristic square-root shape of their dispersion relation (blue lines). The quasienergy dispersion is invariant with respect to shifts by $2\omega_1$ – the reciprocal lattice constant in frequency space. Near q^* , where $\omega_{\text{pl}}(q^*) \approx \omega_1$ holds, the dispersion is strongly altered by the driving (red lines). A gap which hosts non-dispersive modes opens around q^* (yellow shading). The modulation amplitude h is slightly above the instability threshold: damping is negative in a small interval around q^* , leading to an exponential growth of unstable modes (red shading).

we find that the two branches of the plasmon dispersion are given by $\Lambda_-(q) \approx 2i\omega_1 - i\omega_{\text{pl}}(q)/\sqrt{1+h^2/4}$ and $\Lambda_+(q) \approx i\omega_{\text{pl}}(q)/\sqrt{1+h^2/4}$. For Λ_- , we find $\tilde{b}_{\Lambda(q=0)} = -i\tilde{a}_{\Lambda(q=0)}$, giving $\delta\rho_q \approx \tilde{a}_{\Lambda(q)}e^{-i\omega_{\text{pl}}(q)t/\sqrt{1+h^2/4}}$. Therefore, the Λ_- branch is equivalent to a counter-propagating mode with the frequency $-i\omega_{\text{pl}}(q)/\sqrt{1+h^2/4}$ lifted by one reciprocal lattice vector $2\omega_1$.

Furthermore, the periodic driving opens a vertical non-dispersive gap around q^* , where the two branches of the plasmon dispersion meet. Inside the gap, the real part of $\Lambda_{\pm}(q)$ is flat. This phenomenon is known from photonic time varying media, where it is often referred to as momentum-gap or k-gap [68, 69]. The full plasmon dispersion near the onset of the instability ($h\omega_1/4 \gtrsim \gamma/2$) is illustrated in Fig.2.

C. Crystallization

Having identified the wavenumber q^* of the unstable modes in Eqs. (13) and (18), we now study the spatial structure of the plasmon charge density once their initial exponential growth has been cut off by the nonlinear terms of Eq. (11). We focus on a drive and modulation

amplitude yielding h just above the instability threshold, such that the unstable region around q^* is infinitesimally thin. The parametric driving is spatially uniform and cannot supply momentum to the system. Therefore, plasmons can only be created in pairs with wavevectors $\pm\mathbf{q}^*$, where the star indicates that

$$|\mathbf{q}^*| = q^*. \quad (20)$$

We make the assumption that the final steady state to which the system evolves after the onset of the instability will be some linear combination of the original, linearly unstable modes:

$$\delta\rho_s(t, \mathbf{x}) = \cos(\omega_1 t) \sum_{i=1}^N a^{(i)}(t) \cos(\mathbf{q}^{*(i)} \cdot \mathbf{x}) + \sin(\omega_1 t) \sum_{i=1}^N b^{(i)}(t) \cos(\mathbf{q}^{*(i)} \cdot \mathbf{x}). \quad (21)$$

Here, the wave vectors $\mathbf{q}^{*(i)}$ lie on a circle of radius q^* . The nonlinearities of the system determine the ordering pattern reflected in number of wavevectors N in Eq. (21) and their respective angles [70–72]. Typically a roll ($N = 1$), a square lattice ($N = 2$) or a hexagonal lattice ($N = 3$) is formed, depending on the parameters of the system. A similar instability appears in parametrically driven shallow water waves, so called Faraday waves [6–8, 70–73].

For the analysis of pattern formation caused by parametric instabilities, it is sufficient to consider nonlinear terms which project the unstable modes onto themselves [70, 72]. This excludes second order nonlinearities because they give rise to frequency doubling. The third order terms, however, contributes to oscillations at the base frequency ω_1 . Formally, neglecting the second order nonlinearities is equivalent to projecting Eq. (2) onto the restricted subspace of the unstable plane wave modes. Since plasmon modes are longitudinal ($u_{q,j} = \hat{q}_j u_q$) and all wavevectors in Eq. (21) have the length q^* , we can use the linearized continuity equation $-i\omega\delta\rho_q = -\bar{\rho}\hat{q}_i u_{q,i}$, where $\delta\rho_q$, $u_{q,i}$ are single plane wave modes, to approximate

$$u_{s,i} \approx \frac{\omega_1}{q^{*2}} (-i\partial_i) \frac{\delta\rho_s}{\bar{\rho}}. \quad (22)$$

Here, $\delta\rho_s$ is the ansatz of Eq. (21). At this point, it is useful to simplify Eq. (11). Rescaling $\delta\rho_s = h^{1/2}\delta\tilde{\rho}_s$, we find that to order $\mathcal{O}(h)$, the time dependence of m^* in front of the nonlinear terms can be neglected for $h \ll 1$. Thus, with the approximations described above, for the purpose of finding the modulated pattern of the steady state, Eq. (11) is reduced to

$$\partial_t m^*(t) \partial_t \delta\rho_s + \gamma \tilde{m}^* \partial_t \delta\rho_s + \frac{\tilde{m}^* \omega_1^2}{q^{*4} \bar{\rho}^2} \partial_i \partial_j \delta\rho_s \partial_i \delta\rho_s \partial_j \delta\rho_s = 0, \quad (23)$$

where $\delta\rho_s$ is given by Eq. (21) and derivatives act on all functions to their right.

Because in equilibrium the system is rotationally symmetric, we assume that all standing waves in Eq. (21) have equal amplitudes: $a^{(i)} = a$, $b^{(i)} = b$, for all i and with an arbitrary number of modes N included. This is a common assumption in the analysis of pattern formation due to parametric instabilities [70, 72]. A straightforward evaluation of Eq. (23) in which modes lying outside the subspace of unstable modes are neglected leads to amplitude equations

$$\begin{aligned}\dot{a} &= -\alpha b - \frac{1}{2}\gamma a + \beta b(a^2 + b^2) \\ \dot{b} &= -\alpha a - \frac{1}{2}\gamma b - \beta a(a^2 + b^2),\end{aligned}\quad (24)$$

with $\alpha = \omega_1 h/4$ and $\beta = 3\omega_1 \Gamma_N/8(\bar{\rho})^2$, where $\Gamma_N = 2 \left[3(N-1) + 2 \sum_{i=1}^N \cos^2(\vartheta_{\mathbf{q}^{(i)}}) \right]$ and $\vartheta_{\mathbf{q}^{(i)}}$ are the polar angles of the wavevectors $\mathbf{q}^{(i)}$. For $\gamma = 0$, the Eqs. (24) correspond to the equations of motion arising from the Hamiltonian

$$H(a, b) = \frac{1}{2}\alpha(a^2 - b^2) + \frac{1}{4}\beta(a^4 + b^4) + \frac{1}{2}\beta a^2 b^2. \quad (25)$$

The stable minima of the Hamiltonian (25) are located at:

$$a = 0, \quad b = \pm \sqrt{\frac{\alpha}{\beta}}, \quad (26)$$

and their depth is given by $H(\pm\sqrt{\alpha/\beta}, 0) \sim -\Gamma_N^{-1}$. In the presence of weak damping, Eqs. (24) predict that, for any initial condition, the trajectory $\mathbf{r}(t) = (a(t), b(t))$ will descend to one of the minima predicted by Eq. (26) (see Fig. 3). The preferred state will be the one with the deepest minimum. Therefore, the optimal configuration is a charge density wave with

$$N = 1 \quad (27)$$

illustrated in Fig. 1.

It should be noted that our analysis of the crystalline state was carried out for an idealized system. Details of an experimental setup, e.g., boundary conditions, or additional nonlinearities could change the effective Hamiltonian of Eq. (25), making a pattern with $N > 1$ more favorable. The system might also get caught in a local minimum with $N > 1$. In any case, our analysis of the instability indicates that the time and length scales of the resulting structures will be given by q^* and ω_1 .

In what follows, we will assume that the system is in the optimal state with $N = 1$.

IV. COLLECTIVE MODES OF THE NON-EQUILIBRIUM STATE

A. Goldstone-like phonons

The crystalline steady state breaks the rotational and translational symmetries of the system. In the following,

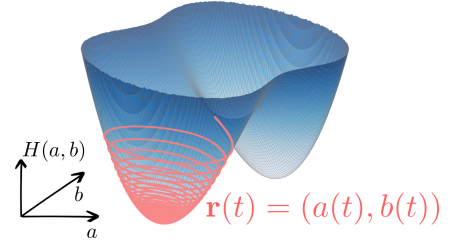


Figure 3. The effective Hamiltonian of Eq. (25) in amplitude space, with the two minima corresponding to symmetry breaking states. The red trajectory is a solution to Eqs. (24) and shows the transition to the crystalline state in the presence of damping.

we show that this symmetry breaking manifests itself in the presence of Goldstone-like phonon modes.

Above, we have found the steady state solution: $\delta\rho = \pm\sqrt{\alpha/\beta}\sin(\omega_1 t)\cos(q^*x)$ (see Eqs. (21), (26)), where for simplicity, we have chosen the x-axis to align with \mathbf{q}^* . The solution remains valid if we shift the phase of the spatial part by φ :

$$\delta\rho = \pm\sqrt{\frac{\alpha}{\beta}}\sin(\omega_1 t)\cos(q^*x + \varphi). \quad (28)$$

If homogeneous and static, the phase shift can always be eliminated by the coordinate transformation $x \rightarrow x - \varphi/q^*$. However, if the phase shift is spatially dependent, Eq. (11) will yield conditions on its dynamics. Thus, we investigate the dynamics of $\varphi(t, \mathbf{x})$, such that the $\delta\rho = \pm A\sin(\omega_1 t)\cos[q^*x + \varphi(t, \mathbf{x})]$ remains an approximate solution to Eq. (11). Since a uniform φ has no influence on the dynamics of the system, we expect slow dynamics for a long wavelength spatial dependence of $\varphi(t, \mathbf{x})$, i.e. we expect Goldstone modes.

To proceed, we write

$$\begin{aligned}\delta\rho &= \frac{A}{2} [\sin(\omega_1 t - q^*x - \varphi(t, \mathbf{x})) \\ &\quad + \sin(\omega_1 t + q^*x + \varphi(t, \mathbf{x}))],\end{aligned}\quad (29)$$

and choose the ansatz

$$\varphi(t, \mathbf{x}) = \varphi_0 e^{-i\Omega t + i\mathbf{Q}\cdot\mathbf{x}} \quad (30)$$

for $\varphi(t, \mathbf{x})$, where

$$\frac{Q}{q^*} \ll 1, \quad \frac{\Omega}{\omega_1} \ll 1. \quad (31)$$

We insert Eq. (29) into Eq. (11) and compare the coefficients in front of the resulting $\sin[\omega_1 t \pm q^*x \pm \varphi(t, \mathbf{x})]$ and $\cos[\omega_1 t \pm q^*x \pm \varphi(t, \mathbf{x})]$ terms in the equations. The equation governing the propagation of the local phase shift $\varphi(t, \mathbf{x})$ follows from the cosine terms. To leading order in $\varphi(t, \mathbf{x})$, Q/q_s and Ω/ω_1 , we find

$$\frac{\partial^2}{\partial t^2}\varphi = \frac{\omega_1^2/q^{*2}}{1+h/2} \left(\left(1 + \frac{11}{4}h\right) \frac{\partial^2}{\partial x^2}\varphi + (1+h) \frac{\partial^2}{\partial y^2}\varphi \right). \quad (32)$$

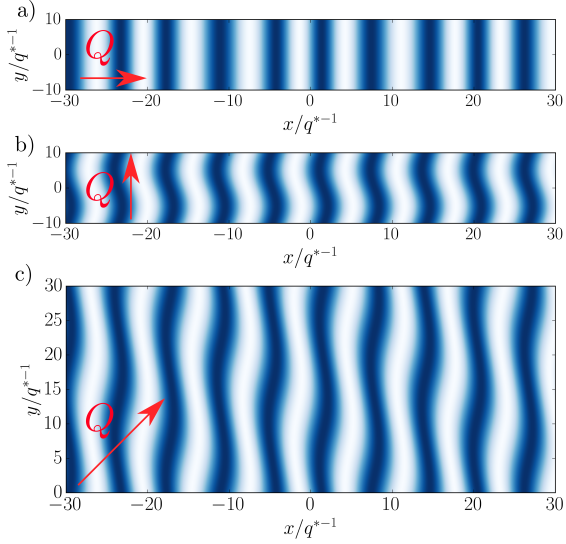


Figure 4. Electron density $\delta\rho$ of Eq. (28) in the presence of the Goldstone-like phonon modes described by Eq. (32). The crystal axis $\hat{\mathbf{q}}^*$ is aligned with the x -axis. The phase $\varphi(t, \mathbf{x})$ propagates in a) x -direction b) y -direction c) in the direction of $(\hat{\mathbf{e}}_x + \hat{\mathbf{e}}_y)/\sqrt{2}$.

The equation obtained from comparing the coefficients in front of the sine terms is fulfilled identically to leading order in Ω/ω_1 .

The dispersion in Eqs. (32) describes soft sound-like modes which can be thought of as the phonons of the crystalline state. Their dispersion

$$\Omega_{\pm} \approx \pm \frac{\omega_1}{q^*} \sqrt{\left(1 + \frac{11}{4}h\right) Q_x^2 + (1+h) Q_y^2} \quad (33)$$

is anisotropic and depends on the magnitude of the Floquet modulation h . Interestingly, similar modes have been observed in parametrically driven classical liquids [74].

B. Optical modes

Besides the Goldstone modes of Eq. (32), the symmetry breaking state supports optical modes. These correspond to oscillations of the amplitudes a , b in the Eqs. (24).

To derive the dispersion of the optical modes, we expand the effective Hamiltonian of Eq. (25) around the minimum at $a = 0$, $b = \sqrt{\alpha/\beta}$:

$$H \approx -\frac{\alpha^2}{4\beta} + \alpha(\delta b^2 + \delta a^2). \quad (34)$$

Then, Hamilton's equations read

$$\begin{aligned} \delta \dot{b} &= 2\alpha \delta a \\ \delta \dot{a} &= -2\alpha \delta b, \end{aligned} \quad (35)$$

and are solved by a uniform oscillation of the amplitudes with the frequency 2α :

$$\delta \ddot{a} + 4\alpha^2 \delta a = 0, \quad (36)$$

with $\alpha = \omega_1 h/4$.

The collective modes of the symmetry broken state described by Eqs. (33) and (36) are one possible experimental signature of the crystalline state. When the dissipation rate γ is included, the modes will obtain a negative imaginary part $\sim -i\gamma$ broadening the resonances.

V. DISCUSSION

Gapped two dimensional Dirac materials are currently an active area of research in material science [75, 76] and promising candidates for Floquet engineering. Recently, ARPES measurements revealed light-induced gaps in black phosphorus [16]. To estimate the experimental feasibility of the proposed setup, we assume typical values for the parameters of our system: $E_g = 0.3$ eV, $\hbar\Omega_F = 0.35$ eV, $\lambda = 15$ eVÅ. Assuming an electron density of $\bar{\rho} = 1.18 \cdot 10^{11}/\text{cm}^{-2}$, such that the chemical potential is close to, but above the resonance, and a plasmon quality factor of $Q = \omega_1/\gamma \approx 10^2$, from the instability condition $h > 2\gamma/\omega_1$, we find the necessary critical amplitude of the electric field to be $\bar{\mathcal{E}} \approx 4 \cdot 10^5$ V/m with a modulation amplitude $\delta\bar{\mathcal{E}} = 0.5\bar{\mathcal{E}}$. The required laser intensity is thus by a factor of 10^4 smaller than in current solid state Floquet engineering experiments [12–14, 16] and generally within the reach of continuous wave lasers. We note that modulated Floquet parametric driving can be used in very different driving regimes. The major limiting factor is the plasmon Q . While quality factors of $Q \approx 1.5 \cdot 10^2$ have been observed in graphene [77], quality factors of up to $10^3 - 10^4$ are believed to be reachable in principle [77, 78]. Such high quality factors would allow to realize the crystalline phase even in a regime where the Floquet base drive frequency is smaller than the gap, $\hbar\Omega_F < E_g$, or to further reduce the necessary laser intensity.

We carried out our calculations using the example of a gapped Dirac material. Another candidate for realizing our ideas is graphene, where light induced gaps have been observed at $\Omega_F = 46$ THz [14].

The crystalline plasmon phase can be detected in multiple ways. Besides the spectroscopic detection of collective Goldstone and optical modes, scanning potentiometry could be used to measure the periodic density $\delta\rho$ of the crystalline state [79, 80]. The plasmon lattice could also be observed through light or electron scattering experiments, where it would act similarly to a 2D grating.

We point out that even for laser intensities below the instability threshold, the propagation of plasmons through a MFPD driven sample will be altered. For example, the opening of the non-dispersive gap in the plasmon dispersion relation can be achieved at sub-critical driving strengths.

From the point of view of applications, modulated Floquet parametric driving offers new possibilities to excite and control THz plasmons by optical or infrared signals. This is promising considering the current interest in efficient THz technology. The crystalline state could be useful in plasmonics, e.g., to construct time-reversal mirrors [81], and for the realization of THz analogues of materials with time varying refractive index [68, 69, 82], which is the subject of an upcoming publication [83]. Finally, we note that similar physics could be implemented using other types of collective modes, e.g., magnons driven by light or high frequency crystal oscillators.

ACKNOWLEDGMENTS

We acknowledge useful conversations with Dmitri Basov, Gaurav K. Gupta and Yiming Pan. E.K. and

N.L. thank the Helen Diller Quantum Center for financial support. N.L. is grateful for funding from the ISF Quantum Science and Technology (2074/19) and from the Defense Advanced Research Projects Agency through the DRINQS program, grant No. D18AC00025. M. R. is grateful to the University of Washington College of Arts and Sciences and the Kenneth K. Young Memorial Professorship for support.

-
- [1] A. Cavalleri, *Photo-induced superconductivity*, Contemporary Physics **59**, 31 (2018).
 - [2] D. Fausti, R. Tobey, N. Dean, S. Kaiser, A. Dienst, M. C. Hoffmann, S. Pyon, T. Takayama, H. Takagi, and A. Cavalleri, *Light-induced superconductivity in a stripe-ordered cuprate*, science **331**, 189 (2011).
 - [3] M. Först, R. Tobey, S. Wall, H. Bromberger, V. Khanna, A. L. Cavalieri, Y.-D. Chuang, W. Lee, R. Moore, W. Schlottner *et al.*, *Driving magnetic order in a manganite by ultrafast lattice excitation*, Physical Review B **84**, 241104 (2011).
 - [4] M. Rini, R. Tobey, N. Dean, J. Itatani, Y. Tomioka, Y. Tokura, R. W. Schoenlein, and A. Cavalleri, *Control of the electronic phase of a manganite by mode-selective vibrational excitation*, Nature **449**, 72 (2007).
 - [5] M. S. Rudner and J. C. Song, *Self-induced berry flux and spontaneous non-equilibrium magnetism*, Nature Physics **15**, 1017 (2019).
 - [6] M. Faraday, *On a peculiar class of acoustical figures; and on certain forms assumed by groups of particles upon vibrating elastic surfaces*, Philosophical transactions of the Royal Society of London (299–340) (1831).
 - [7] T. B. Benjamin and F. J. Ursell, *The stability of the plane free surface of a liquid in vertical periodic motion*, Proceedings of the Royal Society of London. Series A. Mathematical and Physical Sciences **225**, 505 (1954).
 - [8] K. Kumar and L. S. Tuckerman, *Parametric instability of the interface between two fluids*, Journal of Fluid Mechanics **279**, 49 (1994).
 - [9] T. Oka and H. Aoki, *Photovoltaic hall effect in graphene*, Physical Review B **79**, 081406 (2009).
 - [10] T. Kitagawa, T. Oka, A. Brataas, L. Fu, and E. Demler, *Transport properties of nonequilibrium systems under the application of light: Photoinduced quantum hall insulators without landau levels*, Physical Review B **84**, 235108 (2011).
 - [11] N. H. Lindner, G. Refael, and V. Galitski, *Floquet topological insulator in semiconductor quantum wells*, Nature Physics **7**, 490 (2011).
 - [12] Y. Wang, H. Steinberg, P. Jarillo-Herrero, and N. Gedik, *Observation of floquet-bloch states on the surface of a topological insulator*, Science **342**, 453 (2013).
 - [13] F. Mahmood, C.-K. Chan, Z. Alpichshev, D. Gardner, Y. Lee, P. A. Lee, and N. Gedik, *Selective scattering between floquet-bloch and volkov states in a topological insulator*, Nature Physics **12**, 306 (2016).
 - [14] J. W. McIver, B. Schulte, F.-U. Stein, T. Matsuyama, G. Jotzu, G. Meier, and A. Cavalleri, *Light-induced anomalous hall effect in graphene*, Nature physics **16**, 38 (2020).
 - [15] T. Kitagawa, E. Berg, M. Rudner, and E. Demler, *Topological characterization of periodically driven quantum systems*, Physical Review B **82**, 235114 (2010).
 - [16] S. Zhou, C. Bao, B. Fan, H. Zhou, Q. Gao, H. Zhong, T. Lin, H. Liu, P. Yu, P. Tang *et al.*, *Pseudospin-selective floquet band engineering in black phosphorus*, Nature **614**, 75 (2023).
 - [17] G. Usaj, P. M. Perez-Piskunow, L. F. Torres, and C. A. Balseiro, *Irradiated graphene as a tunable floquet topological insulator*, Physical Review B **90**, 115423 (2014).
 - [18] P. M. Perez-Piskunow, G. Usaj, C. A. Balseiro, and L. F. Torres, *Floquet chiral edge states in graphene*, Physical Review B **89**, 121401 (2014).
 - [19] T. Oka and S. Kitamura, *Floquet engineering of quantum materials*, Annual Review of Condensed Matter Physics **10**, 387 (2019).
 - [20] O. Katz, G. Refael, and N. H. Lindner, *Optically induced flat bands in twisted bilayer graphene*, Physical Review B **102**, 155123 (2020).
 - [21] A. Castro, U. De Giovannini, S. A. Sato, H. Hübener, and A. Rubio, *Floquet engineering the band structure of materials with optimal control theory*, Physical Review Research **4**, 033213 (2022).
 - [22] I. Esin, M. S. Rudner, G. Refael, and N. H. Lindner, *Quantized transport and steady states of floquet topological insulators*, Physical Review B **97**, 245401 (2018).
 - [23] I. Esin, M. S. Rudner, and N. H. Lindner, *Floquet metal-to-insulator phase transitions in semiconductor nanowires*, Science advances **6**, eaay4922 (2020).
 - [24] I. Esin, G. K. Gupta, E. Berg, M. S. Rudner, and N. H.

- Lindner, *Electronic floquet gyro-liquid crystal*, Nature communications **12**, 1 (2021).
- [25] H. Dehghani, T. Oka, and A. Mitra, *Out-of-equilibrium electrons and the hall conductance of a floquet topological insulator*, Physical Review B **91**, 155422 (2015).
- [26] M. Genske and A. Rosch, *Floquet-boltzmann equation for periodically driven fermi systems*, Physical Review A **92**, 062108 (2015).
- [27] L. Glazman, *Kinetics of electrons and holes in direct-gap semiconductors photo-excited by high-intensity pulses*, Soviet Physics Semiconductors-USSR **17**, 494 (1983).
- [28] H. Dehghani, T. Oka, and A. Mitra, *Dissipative floquet topological systems*, Physical Review B **90**, 195429 (2014).
- [29] M. Sentef, M. Claassen, A. Kemper, B. Moritz, T. Oka, J. Freericks, and T. Devereaux, *Theory of floquet band formation and local pseudospin textures in pump-probe photoemission of graphene*, Nature communications **6**, 7047 (2015).
- [30] C.-K. Chan, P. A. Lee, K. S. Burch, J. H. Han, and Y. Ran, *When chiral photons meet chiral fermions: photoinduced anomalous hall effects in weyl semimetals*, Physical review letters **116**, 026805 (2016).
- [31] A. Farrell and T. Pereg-Barnea, *Photon-inhibited topological transport in quantum well heterostructures*, Physical Review Letters **115**, 106403 (2015).
- [32] Z. Gu, H. Fertig, D. P. Arovas, and A. Auerbach, *Floquet spectrum and transport through an irradiated graphene ribbon*, Physical review letters **107**, 216601 (2011).
- [33] H. Hübener, M. A. Sentef, U. De Giovannini, A. F. Kemper, and A. Rubio, *Creating stable floquet-weyl semimetals by laser-driving of 3d dirac materials*, Nature communications **8**, 13940 (2017).
- [34] L. Jiang, T. Kitagawa, J. Alicea, A. Akhmerov, D. Pekker, G. Refael, J. I. Cirac, E. Demler, M. D. Lukin, and P. Zoller, *Majorana fermions in equilibrium and in driven cold-atom quantum wires*, Physical review letters **106**, 220402 (2011).
- [35] D. M. Kennes, N. Müller, M. Pletyukhov, C. Weber, C. Bruder, F. Hassler, J. Klinovaja, D. Loss, and H. Schoeller, *Chiral one-dimensional floquet topological insulators beyond the rotating wave approximation*, Physical Review B **100**, 041103 (2019).
- [36] A. Kundu and B. Seradjeh, *Transport signatures of floquet majorana fermions in driven topological superconductors*, Physical review letters **111**, 136402 (2013).
- [37] M. Thakurathi, D. Loss, and J. Klinovaja, *Floquet majorana fermions and parafermions in driven rashba nanowires*, Physical Review B **95**, 155407 (2017).
- [38] D. V. Else, B. Bauer, and C. Nayak, *Floquet time crystals*, Physical review letters **117**, 090402 (2016).
- [39] N. Y. Yao, A. C. Potter, I.-D. Potirniche, and A. Vishwanath, *Discrete time crystals: Rigidity, criticality, and realizations*, Physical review letters **118**, 030401 (2017).
- [40] A. Kyprianidis, F. Machado, W. Morong, P. Becker, K. S. Collins, D. V. Else, L. Feng, P. W. Hess, C. Nayak, G. Pagano *et al.*, *Observation of a prethermal discrete time crystal*, Science **372**, 1192 (2021).
- [41] J. Zhang, P. W. Hess, A. Kyprianidis, P. Becker, A. Lee, J. Smith, G. Pagano, I.-D. Potirniche, A. C. Potter, A. Vishwanath *et al.*, *Observation of a discrete time crystal*, Nature **543**, 217 (2017).
- [42] S. Choi, J. Choi, R. Landig, G. Kucsko, H. Zhou, J. Isoya, F. Jelezko, S. Onoda, H. Sumiya, V. Khemani *et al.*, *Observation of discrete time-crystalline order in a disordered dipolar many-body system*, Nature **543**, 221 (2017).
- [43] A. Lazarides, A. Das, and R. Moessner, *Equilibrium states of generic quantum systems subject to periodic driving*, Physical Review E **90**, 012110 (2014).
- [44] L. D'Alessio and M. Rigol, *Long-time behavior of isolated periodically driven interacting lattice systems*, Physical Review X **4**, 041048 (2014).
- [45] M. Bukov, M. Heyl, D. A. Huse, and A. Polkovnikov, *Heating and many-body resonances in a periodically driven two-band system*, Physical Review B **93**, 155132 (2016).
- [46] M. Bukov, L. D'Alessio, and A. Polkovnikov, *Universal high-frequency behavior of periodically driven systems: from dynamical stabilization to floquet engineering*, Advances in Physics **64**, 139 (2015).
- [47] D. V. Else, B. Bauer, and C. Nayak, *Prethermal phases of matter protected by time-translation symmetry*, Physical Review X **7**, 011026 (2017).
- [48] T. Mori, *Floquet prethermalization in periodically driven classical spin systems*, Physical Review B **98**, 104303 (2018).
- [49] M. Reitter, J. Näger, K. Wintersperger, C. Sträter, I. Bloch, A. Eckardt, and U. Schneider, *Interaction dependent heating and atom loss in a periodically driven optical lattice*, Physical review letters **119**, 200402 (2017).
- [50] K. Singh, C. J. Fujiwara, Z. A. Geiger, E. Q. Simmons, M. Lipatov, A. Cao, P. Dotti, S. V. Rajagopal, R. Senaratne, T. Shimasaki *et al.*, *Quantifying and controlling prethermal nonergodicity in interacting floquet matter*, Physical Review X **9**, 041021 (2019).
- [51] V. Galitsky, S. Goreslavsky, and V. Elesin, *Electric and magnetic properties of a semiconductor in the field of a strong electromagnetic wave*, SOV PHYS JETP **30**, 117 (1970).
- [52] T. Shirai, T. Mori, and S. Miyashita, *Condition for emergence of the floquet-gibbs state in periodically driven open systems*, Physical Review E **91**, 030101 (2015).
- [53] K. I. Seetharam, C.-E. Bardyn, N. H. Lindner, M. S. Rudner, and G. Refael, *Controlled population of floquet-bloch states via coupling to bose and fermi baths*, Physical Review X **5**, 041050 (2015).
- [54] T. Iadecola, T. Neupert, and C. Chamon, *Occupation of topological floquet bands in open systems*, Physical Review B **91**, 235133 (2015).
- [55] K. I. Seetharam, C.-E. Bardyn, N. H. Lindner, M. S. Rudner, and G. Refael, *Steady states of interacting floquet insulators*, Physical Review B **99**, 014307 (2019).
- [56] D. E. Liu, *Classification of the floquet statistical distribution for time-periodic open systems*, Physical Review B **91**, 144301 (2015).
- [57] D. A. Abanin, W. De Roeck, and F. Huveneers, *Exponentially slow heating in periodically driven many-body systems*, Physical review letters **115**, 256803 (2015).
- [58] A. Eguiluz and J. Quinn, *Hydrodynamic model for surface plasmons in metals and degenerate semiconductors*, Physical Review B **14**, 1347 (1976).
- [59] D. Pines and P. Nozières, *Theory Of Quantum Liquids: Normal Fermi Liquids*, CRC Press (1989). ISBN 978-0201407747.
- [60] U. Briskot, M. Schütt, I. V. Gornyi, M. Titov, B. N. Narozhny, and A. D. Mirlin, *Collision-dominated nonlinear hydrodynamics in graphene*, Phys. Rev. B **92**, 115426 (2015).

- [61] D. Forster, *Hydrodynamic Fluctuations, Broken Symmetry, and Correlation Functions*, CRC Press (2018). ISBN 978-0367091323.
- [62] L. D. Landau and E. M. Lifshits, *Fluid mechanics*, Butterworth-Heinemann (1987). ISBN 978-0750627672.
- [63] A. Lucas and S. Sachdev, *Memory matrix theory of magnetotransport in strange metals*, Physical Review B **91**, 195122 (2015).
- [64] L. D. Landau and E. M. Lifshitz, *Mechanics*, Butterworth-Heinemann (1976). ISBN 978-0750628969.
- [65] A. Lucas and S. D. Sarma, *Electronic sound modes and plasmons in hydrodynamic two-dimensional metals*, Phys. Rev. B **97**, 115449 (2018).
- [66] E. I. Kiselev, *Universal superdiffusive modes in charged two dimensional liquids*, Physical Review B **103**, 235116 (2021).
- [67] The Fourier transform of the Coulomb potential is $V(q) = 2\pi/q$ and is responsible for the characteristic $\sim \sqrt{q}$ dispersion of two dimensional plasmons, whereas the pressure term scales as $\sim q$ and will only contribute a small correction.
- [68] E. Galiffi, R. Tirole, S. Yin, H. Li, S. Vezzoli, P. A. Huidobro, M. G. Silveirinha, R. Sapienza, A. Alù, and J. Pendry, *Photonics of time-varying media*, Advanced Photonics **4**, 014002 (2022).
- [69] M. Lyubarov, Y. Lumer, A. Dikopoltsev, E. Lustig, Y. Sharabi, and M. Segev, *Amplified emission and lasing in photonic time crystals*, Science (eabo3324) (2022).
- [70] P. Chen and J. Vinals, *Amplitude equation and pattern selection in faraday waves*, Physical Review E **60**, 559 (1999).
- [71] P. Chen and J. Vinals, *Pattern selection in faraday waves*, Physical Review Letters **79**, 2670 (1997).
- [72] H. W. Müller, *Model equations for two-dimensional quasipatterns*, Physical Review E **49**, 1273 (1994).
- [73] W. S. Edwards and S. Fauve, *Patterns and quasi-patterns in the faraday experiment*, Journal of Fluid Mechanics **278**, 123 (1994).
- [74] L. Domino, M. Tarpin, S. Patinet, and A. Eddi, *Faraday wave lattice as an elastic metamaterial*, Physical Review E **93**, 050202 (2016).
- [75] A. Chaves, J. G. Azadani, H. Alsalman, D. Da Costa, R. Frisenda, A. Chaves, S. H. Song, Y. D. Kim, D. He, J. Zhou *et al.*, *Bandgap engineering of two-dimensional semiconductor materials*, npj 2D Materials and Applications **4**, 1 (2020).
- [76] A. Chaves, R. Ribeiro, T. Frederico, and N. Peres, *Excitonic effects in the optical properties of 2d materials: an equation of motion approach*, 2D Materials **4**, 025086 (2017).
- [77] G. Ni, d. A. McLeod, Z. Sun, L. Wang, L. Xiong, K. Post, S. Sunku, B.-Y. Jiang, J. Hone, C. R. Dean *et al.*, *Fundamental limits to graphene plasmonics*, Nature **557**, 530 (2018).
- [78] A. Principi, G. Vignale, M. Carrega, and M. Polini, *Intrinsic lifetime of dirac plasmons in graphene*, Physical Review B **88**, 195405 (2013).
- [79] Z. J. Krebs, W. A. Behn, S. Li, K. J. Smith, K. Watanabe, T. Taniguchi, A. Levchenko, and V. W. Brar, *Imaging the breaking of electrostatic dams in graphene for ballistic and viscous fluids*, Science **379**, 671 (2023).
- [80] R. Möller, U. Albrecht, J. Boneberg, B. Koslowski, P. Leiderer, and K. Dransfeld, *Detection of surface plasmons by scanning tunneling microscopy*, Journal of Vacuum Science & Technology B: Microelectronics and Nanometer Structures Processing, Measurement, and Phenomena **9**, 506 (1991).
- [81] V. Bacot, G. Durey, A. Eddi, M. Fink, and E. Fort, *Phase-conjugate mirror for water waves driven by the faraday instability*, Proceedings of the National Academy of Sciences **116**, 8809 (2019).
- [82] E. Lustig, Y. Sharabi, and M. Segev, *Topological aspects of photonic time crystals*, Optica **5**, 1390 (2018).
- [83] E. I. Kiselev and Y. Pan, *unpublished*.